doi:10.1093/brain/awq145 Brain 2010: 133; 2331–2347 | 2331

BRAIN
A JOURNAL OF NEUROLOGY

Animals lacking link protein have attenuated perineuronal nets and persistent plasticity

Daniela Carulli,[1,2] Tommaso Pizzorusso,[3,4] Jessica C. F. Kwok,[1] Elena Putignano,[3] Andrea Poli,[5] Serhiy Forostyak,[6] Melissa R. Andrews,[1] Sathyaseelan S. Deepa,[1] Tibor T. Glant[7] and James W. Fawcett[1]

1 Cambridge University Centre for Brain Repair, Department of Clinical Neurosciences, University of Cambridge, Robinson Way, Cambridge, CB2 0PY, UK
2 Scientific Institute of the Cavalieri-Ottolenghi Foundation, A.O. San Luigi Gonzaga, Regione Gonzole 10, 10043 Orbassano, TO, Italy
3 Neuroscience Institute CNR, Area Ricerca CNR, via Moruzzi, 1 Pisa 56125, Italy
4 Department of Psychology, University of Florence, Padiglione 26 Area San Salvi, 50135 Florence, Italy
5 Scuola Normale Superiore, Neurobiology Laboratory, Area Ricerca CNR via Moruzzi, 1 Pisa 56125, Italy
6 Department of Neuroscience, Laboratory of Tissue Culture and Stem Cells, Institute of Experimental Medicine, Academy of Sciences of the Czech Republic, Videnska 1083, 142 20, Prague 4, Czech Republic
7 Section of Molecular Medicine, Department of Orthopaedic Surgery, Rush University Medical Centre, Chicago, IL 60612, USA

Correspondence to: James Fawcett,
Cambridge University Centre for Brain Repair,
Robinson Way, Cambridge CB2 0PY, UK
E-mail: jf108@cam.ac.uk

Chondroitin sulphate proteoglycans in the extracellular matrix restrict plasticity in the adult central nervous system and their digestion with chondroitinase reactivates plasticity. However the structures in the extracellular matrix that restrict plasticity are unknown. There are many changes in the extracellular matrix as critical periods for plasticity close, including changes in chondroitin sulphate proteoglycan core protein levels, changes in glycosaminoglycan sulphation and the appearance of dense chondroitin sulphate proteoglycan-containing perineuronal nets around many neurons. We show that formation of perineuronal nets is triggered by neuronal production of cartilage link protein Crtl1 (Hapln1), which is up-regulated in the visual cortex as perineuronal nets form during development and after dark rearing. Mice lacking Crtl1 have attenuated perineuronal nets, but the overall levels of chondroitin sulphate proteoglycans and their pattern of glycan sulphation are unchanged. Crtl1 knockout animals retain juvenile levels of ocular dominance plasticity and their visual acuity remains sensitive to visual deprivation. In the sensory pathway, axons in knockout animals but not controls sprout into the party denervated cuneate nucleus. The organization of chondroitin sulphate proteoglycan into perineuronal nets is therefore the key event in the control of central nervous system plasticity by the extracellular matrix.

Keywords: plasticity; ocular dominance; extracellular matrix; proteoglycan; GABA; interneurons; synapse; link protein
Abbreviations: ChABC = chondroitinase ABC; CSPG = chondroitin sulphate proteoglycan; PNN = perineuronal net

Introduction

Some functional recovery occurs after damage to the CNS, mainly through axonal sprouting, dendritic remodelling and changes in neuronal properties and synaptic strength, known collectively as plasticity. Recovery can be further enhanced by influencing plasticity through rehabilitation (Girgis *et al.*, 2007; Fawcett and Curt, 2009; Garcia-Alias *et al.*, 2009). This process can be enhanced in

Received April 3, 2010. Revised April 27, 2010. Accepted April 29, 2010. Advance Access publication June 20, 2010

the adult CNS by treatment with chondroitinase ABC (ChABC) (reviewed in Kwok *et al.,* 2008). ChABC digests the glycosaminoglycan chains on chondroitin sulphate proteoglycans (CSPGs). However, CSPGs participate in many structures in the extracellular matrix, and the ChABC-induced change that affects plasticity has not been identified. An approach to finding out how CSPGs control plasticity is to find out how they turn it off during development. Late in development, connections in the mammalian CNS go through a period, known as the critical period, during which they are highly malleable. In the visual cortex, the critical period closes at around 5 years in humans, 12 weeks in kittens and 35 days in mice (Gordon and Stryker, 1996), after which the capacity for experience-dependant change is much reduced through several mechanisms (Blakemore and Van Sluyters, 1974; Sawtell *et al.,* 2003; Sengpiel, 2007; Lehmann and Lowel, 2008; Morishita *et al.,* 2008; Sato *et al.,* 2008). There are similar plastic periods in other parts of the CNS. Ocular dominance and other forms of plasticity can be reactivated in adult animals by digestion of CSPGs with ChABC (Pizzorusso *et al.,* 2002; Tropea *et al.,* 2003; Barritt *et al.,* 2006; Massey *et al.,* 2006; Curinga *et al.,* 2007; Galtrey *et al.,* 2007; Cafferty *et al.,* 2008; Garcia-Alias *et al.,* 2009; Houle *et al.,* 2009) allowing the CNS to show improved recovery from amblyopia, spinal cord injury and other conditions. ChABC treatment also affects memory formation and retention in adult animals, indicating a role for CSPGs in these processes (Gogolla *et al.,* 2009). These and other observations have led to the view that CSPGs in the extracellular matrix are involved in the control of CNS plasticity and the termination of critical periods. It is not clear which of many events involving CSPGs is responsible for the reduction in plasticity at the end of the critical periods. There are three main changes. First, there are seven or more CSPG core proteins whose levels change during postnatal development and following injury. Second, the sulphation motifs on the glycosaminoglycans change during development and following damage, and their pattern determines most of the binding properties and actions of CSPGs (Kitagawa *et al.,* 1997; Properzi *et al.,* 2005; Busch *et al.,* 2007; Iaci *et al.,* 2007; Massey *et al.,* 2008; Wang *et al.,* 2008). Third, at the end of the critical periods some CSPGs that were previously diffusely distributed are incorporated into specialized structures of condensed and stable matrix around the somata and dendrites of neurons, known as perineuronal nets (PNNs) (Hockfield *et al.,*1990; Schweizer *et al.,* 1993; Pizzorusso *et al.,* 2002; Galtrey *et al.,* 2008). ChABC digestion leads to many extracellular matrix changes: glycosaminoglycans are digested to disaccharides, glycosaminoglycan-bound molecules are released, CSPG levels change, neurocan is completely removed and PNNs are partly demolished. Based on this evidence, one can hypothesize that the reduction in plasticity at the end of critical periods could be due to a change in the level of one or more of the CSPG core proteins, to a change in the pattern of glycosaminoglycan sulphation or to the localization of CSPGs in PNNs. Attention has focused on PNNs (Massey *et al.,* 2006; Busch and Silver, 2007; Dityatev *et al.,* 2007; McRae *et al.,* 2007; Bruckner *et al.,* 2008; Morishita and Hensch, 2008; Tropea *et al.,* 2008; Frischknecht *et al.,* 2009) because they are readily seen and because many surround parvalbumin positive GABAergic interneurons, which are involved in the control and restriction of plasticity (Schweizer *et al.,* 1993; Pizzorusso *et al.,* 2002; Fagiolini *et al.,* 2004; Hofer *et al.,* 2006; Tropea *et al.,* 2008). Moreover, sensory deprivation by dark rearing, whisker removal or song deprivation in birds delays PNN formation in the visual cortex, somatosensory cortices and high vocal centre, respectively (Pizzorusso *et al.,* 2002; McRae *et al.,* 2007; Balmer *et al.,* 2009; Nakamura *et al.,* 2009). Also, promoting plastic change in adults through environmental enrichment or pharmacological treatment decreases the number of PNNs (Sale *et al.,* 2007; Harauzov *et al.,* 2010). There is therefore a correlation between the ability of the cortex to undergo plastic change and the presence of PNNs. However, proof that PNNs rather than other changes in CSPGs control plasticity, and whether ChABC reactivates plasticity by removing PNNs, is lacking.

In this article we have measured the changes in the CSPGs that occur during the critical period in rats and mice. We have identified the molecular event that triggers PNN formation, showing that the PNN component cartilage link protein Crtl1 (Hapln1) is up-regulated as the structures form, and that animals lacking link protein in the CNS have very attenuated PNNs. In keeping with the hypothesis that PNN maturation down-regulates plasticity, we found that adult plasticity in the visual and somatosensory systems of mice lacking Crtl1 was strongly enhanced. These findings provide direct evidence that PNNs control plasticity in the CNS and suggest that digestion of these structures is how ChABC reactivates CNS plasticity.

Materials and methods

Animals

Postnatal Day 3, 7, 14, 21, 35 and adult (~3-month-old) Sprague-Dawley rats (Charles River, Margate, UK), adult (>13-week-old) C57/Bl6 (Charles River, Margate, UK) and Crtl1 knockout mice were used in this study. All procedures were performed in compliance with the UK Animals (Scientific Procedures) Act 1986 and institutional guidelines, and the Italian law for care and use of experimental animals (DL116/92).

Histochemistry

Animals were perfused with cold 4% paraformaldehyde and post-fixed overnight. Thirty micrometre sections were blocked in 3% goat or donkey serum 3% bovine serum albumin, in Tris buffered saline with 0.2% triton X-100. *Wisteria floribunda* agglutinin and hyaluronan binding protein histochemistry was performed by incubating sections in biotinylated *W. floribunda* agglutinin (20 μg/ml, Sigma, Haverhill, UK) or biotinylated hyaluronan binding protein (10 μg/ml, Seikagaku, Falmouth, MA, USA) for 2 h room temp, then in ABC solution (ABC Elite Kit, Vector, Peterborough, UK) for 1 h room temperature and in diaminobenzidine (0.5 mg/ml in Tris non-saline with 0.3 μl/ml H_2O_2) for 5–10 min room temperature. For immunohistochemistry, the antibodies are shown in Table 1. For aggrecan immunolabelling, sections were pre-incubated with chondroitinase ABC (0.02 U/ml, Seikagaku).

Table 1 List of the antibodies used in this study

Antibodies	Supplier	Species of origin	Dilution	
			Immunohistochemistry	Western blotting
a-Crtl1	R&D Systems (Minneapolis, MN, USA)	Goat	1:100	1:1000
a-neurocan-N PAb 291	Dr A. Oohira	Rabbit	1:500	1:2000
a-aggrecan	Chemicon (Temecula, CA, USA)	Rabbit	1:500	1:1500
a-brevican	Dr C. Seidenbecher	Rabbit	1:4000	1:10 000
a-versican	Chemicon	Rabbit	1:500	1:2000
a-phosphacan 3F8	DSHB (Iowa City, IA, USA)	Mouse	1:100	1:50
a-tenascin-R	Dr P. Pesheva	Rabbit	1:2000	1:10 000
a-parvalbumin	Swant (Swant, Bellinzona, Switzerland)	Rabbit	1:2000	–

For each antibody, the supplier, the species of origin and the dilutions are reported.
DSHB = Developmental Study Hybridoma Bank.

Table 2 Primer sequences and polymerase chain reaction product size

Molecule	Forward primer (5′–3′)	Reverse primer (5′—3′)	PCR product size
Neurocan	ctgcttctttacccttcaaccac	agttgtcaaagccatcttcgaac	443 bp (247–689)
Brevican	cctcaggaagctgtggagag	cttgccccatctggagtaga	452 bp (1271–1722)
Aggrecan	ggccttccctctggatttag	gccagaagaatctccactgc	663 bp (2350–3012)
Phosphacan	ggtcttcaaggcaagcaaaa	agctggctttcagagatgct	423 bp (462–884)
RPTPbeta	acaccaccaacacccatctt	taggcgtccactggatcttc	621 bp (5158–5778)
VersicanV2	aacacagcaccctctgacaa	gcacaggtgcacacatagga	321 bp (808–1128)
TN-R	cttccagctacaacacatcc	acacattccccatccacac	601 bp (152–752)
Crtl1	cccttactttccacgattgg	atctgggaaacccacaaagc	535 bp (483–1017)
Bral2	tcgcctcttcggtgtctact	gaccaaggaccacaacaggt	356 bp (1062–1417)
HAS1	ctctggactcttgggtcagc	cagccacaaagaaagggaag	435 bp (872–1306)
HAS2	ggcaccttaccaacagggta	taaaccacacggacactgga	513 bp (1450–1962)
HAS3	cttctttgtgtggcgtagca	tcaggactcggttggtaagg	536 bp (615–1150)

The specific cDNA sequence amplified by polymerase chain reaction (PCR) is indicated in brackets near the polymerase chain reaction product size.
TN-R = tenascin-R; HAS = hyaluronan synthase.

Synthesis of probes for *in situ* hybridization

RNA from adult rat brain was isolated by guanidinium thiocyanate phenol/chloroform extraction. For dig-labelled RNA probes, a first-strand cDNA was synthesized. The primer sequences etc. are shown in Table 2. The polymerase chain reaction product was amplified using a 5′ primer containing a T7 phage promoter sequence and a 3′ primer containing a SP6 phage promoter sequence, generating a template for transcription of a sense and an antisense probe. *In vitro* transcription reaction was performed using dig-UTP RNA labelling mix (Roche, Mannheim, Germany) and SP6 or T7 RNA polymerase (Roche).

In situ hybridization

Fourteen micrometre sections from fresh-frozen brain were collected on Superfrost slides and air-dried. After fixation, slides underwent fixation in 4% paraformaldehyde, permeabilization in phosphate buffered saline 0.5% Triton X-100 acetylation for 10 min 250 ml water, 3.5 ml triethanolamine, 625 µl acetic anhydrid. Prehybridization was in 50% formamide, 5× saline sodium citrate and 2% blocking reagent (Roche) for 3 h room temperature. Hybridization with dig-labelled probes (100 ng/ml) took place overnight, in the same buffer at 69°C. Stringency washing was in 0.2× saline sodium citrate for 1 h at 69°C. For the detection of hybrids, slides were equilibrated in maleic acid buffer (0.1 M maleic acid and 0.15 M NaCl, pH 7.5), incubated for 1 h room temperature with 1% blocking reagent made in maleic acid buffer and 1 h with alkaline phosphatase-conjugated anti-dig antibodies (Roche) diluted 1:5000 in blocking buffer. The slides were washed and incubated overnight in 2.4 mg levamisole (Sigma), 45 µl 4-nitroblue tetrazolium (Sigma) and 35 µl 5-bromo-4-chloro-3-indolyl-phosphate (Sigma) in 10 ml of a buffer made of 0.1 M Trizma base, 0.1 M NaCl and 0.005 M $MgCl_2$, pH 9.5. The colour development reaction was stopped in 0.01 M Trizma base and 0.001 M EDTA, pH 8.

For Kv3.1b immunofluorescence, sections were incubated in rabbit anti-Kv3.1b antibodies for 1 h room temperature. They were then incubated in biotinylated donkey anti-rabbit antibodies (1:500, Amersham) for 1 h room temperature and in Cy3 streptavidin (1:500, Amersham) for 45 min room temperature.

Quantitative reverse transcriptase-polymerase chain reaction

RNA from visual cortex was isolated by acid guanidinium thiocyanate phenol/chloroform extraction, a first-strand cDNA was synthesized

from 1 μg of RNA, using a cDNA synthesis kit from Invitrogen. Quantitative polymerase chain reaction was carried out using ABI Prism 7000 Sequence Detection System instrumentation (Applied Biosystems) in combination with Taqman reagent-based chemistry (Applied Biosystems) to determine the amount of Crtl1 relative to beta-actin at the different developmental time points.

Extraction of proteoglycans from mouse brain and western blotting

Tissue dissected from the region of the visual cortex was homogenized with a Potter homogenizer using 5 ml/brain extraction buffer [50 mM Tris buffered saline (pH 7.0), 2 mM EDTA, 10 mM *N*-ethylmaleimide and 2 mM phenylmethylsulphonylfluoride as protease inhibitors (Buffer 1)]. The homogenate was centrifuged at 15 000 rpm for 30 min, at 4°C. The supernatant was collected and the pellet re-extracted twice with Buffer 1. The supernatants (Tris buffered saline extract) were pooled together. The pellet obtained after centrifugation was further extracted three times with Buffer 2 (Buffer 1 containing 0.5% Triton X-100), followed by extraction with Buffer 3 (Buffer 2 containing 6 M urea). The 6 M urea extract was dialysed against phosphate buffered saline. Two hundred micrograms protein was precipitated with 95% ethanol/1.3% potassium acetate for 1 h in ice, and the precipitate recovered by centrifugation at 15 000rpm for 10 min and digested with 10 ChABC. The digests were subjected to sodium dodecyl sulphate polyacrylamide gel electrophoresis in 5% gel under reducing conditions and electrotransfered (Hybond-C pure, Amersham). The membrane was blocked, incubated with primary antibodies, washed and then incubated with peroxidase-conjugated anti-rabbit or anti-goat immunoglobulin G (1:10 000, Vector). The membrane was then developed using chemiluminescent substrate (ECL, Amersham).

Glycosaminoglycan purification

Cortices were homogenized with chilled acetone and dried before being suspended in 0.1 M Tris–Ac, 10 mM calcium acetate, pH 7.8 and digested with pronase overnight. After centrifugation, 100% trichloroacetic acid was added to the supernatant, centrifuged and the supernatant collected. After addition of diethyl ether, residual ether was allowed to evaporate. Glycosaminoglycan was precipitated with 5% sodium acetate and 75% cold ethanol, centrifuged and dried. For analysis of disaccharide composition, the glycosaminoglycan was digested with 100 mU ChABC in 100 mM NH_4Ac buffer, pH 8.0 for 16 h at 37°C.

Analysis of glycosaminoglycans using fluorophore-assisted carbohydrate electrophoresis

Procedures for 2-aminoacridone-derivatization of the disaccharides were modified from Calabro *et al.* (2001). Dried experimental and standard disaccharide preparations were derivatized with 12.5 mM 2-aminoacridone in the presence of 10 μl of 1.25 M sodium cyanoborohydride at 37°C overnight. Samples were electrophoresed in a 30% polyacrylamide gel in 0.1 M Tris–borate buffers, pH 8.3, then imaged at 365 nm.

Quantitation

In situ hybridization

Quantitation was performed as in previous papers (Carulli *et al.*, 2006, 2007; Galtrey *et al.*, 2008). For the study of expression levels during development, optical density (greyscale levels of the corresponding pixels of the pre-processed image) of selected visual cortex neurons was recorded by means of Lucia software (Nikon) under a 40× objective. The mean optical density for each neuron (20–30 neurons/animal) was measured and the background level from a non-stained region subtracted. The mean level was calculated for each animal and the measurements obtained for each were pooled to yield the final mean values (±SD). For quantification of PNN components after dark rearing, neurons were classified into dark, medium and light stains, and the number of each type was counted in 350 × 140 μm areas drawn in the appropriate layers of the cortex. Each estimation was the mean of at least eight measurements in each of three animals.

For quantitation of CSPG core protein levels, images were taken from five different views of layers 2–4 of the visual cortex in five sections per animal; three animals were used for each time point. The optical density (greyscale levels of the corresponding pixels of the pre-processed image) of selected rat cortex was measured using ImageJ (ver 1.42q; NIH, USA). The mean level was calculated for each animal and the measurements obtained from each were pooled to yield the final mean values. The background optical density from alternate cortical sections, without the addition of primary antibody, was subtracted.

Quantitation of perineuronal nets

An area of interest was drawn around the immunopositive region of individual neurons with full or attenuated *W. floribunda* agglutinin-stained PNNs (Fig. 5c and d). The area of each region of interest and the brightness of fluorescence (on a 0–256 scale) was measured by means of Neurolucida software under a 40× objective. The background brightness, taken from a non-stained region of cortex, was subtracted from the brightness measurement. Each measurement was the mean of at least 50 measurements in each of four animals.

Quantitation of parvalbumin neurons

For measurements of the area and the perimeter of the neurons, the outline of the soma was drawn around 30 neurons in each of three animals. The number of parvalbumin neurons in 490 × 700 μm areas of interest were counted and the percentage of parvalbumin neurons that were surrounded by a *W. floribunda* agglutinin-positive PNN were counted from 245 × 665 μm areas of interest, spanning all cortical layers. The number of primary dendrites was counted on parv-stained neurons. Each estimation was the mean of at least seven measurements in each of three animals.

Electrophysiological analysis of ocular dominance

The age of mice ranged from postnatal Day 91 up to postnatal Day 120. Mice were backcrossed for seven generations into C57BL6J background. Experiments were performed blind to genotype in urethane anaesthetized mice (20% in saline; 6 ml/kg i.p.). Visual evoked potentials were recorded as described (Putignano *et al.*, 2007), by means of a micropipette (2–2.5 M impedance) inserted into the binocular portion of the primary visual cortex (Oc1B). Only penetrations in which single-cell receptive fields were within 20° of the vertical meridian were used to assess visual evoked potential acuity.

To record visual evoked potentials, the electrode was positioned at a depth of 450–500 μm; at this depth, visual evoked potentials had their maximal amplitude. Signals were bandpass filtered (0.1–100 Hz), amplified and fed to a computer for analogue-to-digital conversion (512 Hz) and analysis. Signals were averaged for at least 128 events in blocks of 16 events, each in synchrony with the stimulus contrast reversal. Transient visual evoked potentials in response to abrupt contrast reversal (1 Hz) were evaluated in the time domain by measuring the peak-to-trough amplitude and peak latency of the major negative component. Visual stimuli were horizontal sinusoidal gratings of different spatial frequency and contrast generated by a VSG2/2 card (Cambridge Research System) by custom software and presented on the face of a monitor (20 × 22 cm; luminance, 15 cd/m^2) positioned 20 or 30 cm from the mouse's eyes and centred on the previously determined receptive fields. Visual acuity was obtained by extrapolation of the linear regression to zero amplitude through the last four data points above noise level in a curve where visual evoked potential amplitude is plotted against log spatial frequency (Pizzorusso *et al.*, 2006).

Transgenic mice lacking expression of Crtl1 in the adult CNS

The development of this animal is described by Czipri *et al.* (2003). Gene targeting was performed by disrupting exon 4 of the *Crtl1* gene upstream of the hyaluronan-binding 'link module' by the pGK-neo^r-poly(A) cassette in the pPNT vector.

To generate transgenic mice that overexpress Crtl1 in cartilage, a 1758 base-pair cDNA fragment containing the entire coding sequence was inserted into the transgenic vector pSP/44-3. Linearized and purified transgenic construct was microinjected into fertilized egg cells (DNX Technologies, Princeton, NJ). *Crtl1*-deficient (*Crtl1*$^{-/-}$) and *Crtl1*-transgenic (*Crtl1-Tg*) mice were inter-crossed to achieve a *Crtl1*$^{-/-}$/*Crtl1-Tg*$^{+/+}$ state. The original Crtl1$^{-/-}$/Crtl1-Tg$^{+/+}$ mice were in a BALB/C background. For ocular dominance experiments they were bred into the pigmented C57BL/6 background.

Plasticity in the cuneate nucleus

Age matched adult male (2–4 months) link protein 1 knockout mice or CD1 mice (Charles River Laboratories) were anaesthetized, then unilateral dorsal spinal hemisection was performed on the right side between the dorsal roots of C6 and C7 ($n = 7$, link protein 1 knockout; $n = 12$, CD1 mice). One week after injury, the forepaw innervation of the cuneate nucleus was traced using 1–2 μl of cholera toxin B subunit (1%, List Biological Laboratories; Campbell, CA) injected subcutaneously into the palmer side of each digit and into the glaborous foot pad of the right forepaw. Two weeks post-injury and one week post-tracing, animals were killed and perfused with 4% paraformaldehyde (pH 7.4). Twenty-micrometre thick cryostat sections were immunostained as above. Primary antibodies were anti-cholera toxin B (1:2000, goat, List Biological Laboratories; Campbell, CA) and anti-glial fibrillary acidic protein (1:400, mouse, Sigma).

Quantitation of sprouting in the right cuneate nucleus was performed in each animal by examining six sections (160 μm apart) throughout the length of the nucleus and measuring the area of cholera toxin B labelling. A perimeter was drawn around the cholera toxin B-traced afferents and measurements were taken in micrometre square. Average areas of cholera toxin B tracing from each animal were combined to calculate group averages (either link protein 1 knockout or CD1 control), which were analysed using one-way ANOVA.

Results

Developmental changes in CSPG core proteins and glycosaminoglycans

Previous biochemical quantifications of CSPG core protein levels have shown large developmental changes in the CNS. In order to confirm that the same changes occur in the visual cortex, we used quantitative immunostaining of layers 2–4 of the rat visual cortex (as used for previous experiments on ChABC and ocular dominance). The changes we measured agree closely with those seen in previous studies of the whole rat brain (Milev *et al.*, 1998; Zimmermann and Dours-Zimmermann, 2008). Aggrecan, brevican and versican V2 levels increased and neurocan decreased over the critical period (Fig. 1a–d). Many of the binding interactions of CSPGs are via their glycosaminoglycans, with different sulphation motifs having different binding specificities (Sugahara *et al.*, 2003). Previous studies have shown changes in sulphation patterns between birth and adulthood. We compared glycosaminoglycan sulphation in the cortex at birth, postnatal Day 21 (beginning of the critical period) and adulthood. Strikingly, the sulphation pattern of CSPGs was very similar at postnatal Days 21 and 0, and the main changes were between postnatal Day 21 and adulthood, at which time there was virtual disappearance of 6-sulphated glycosaminoglycan and an increase in 4-sulphated glycosaminoglycan, with falls in the two disulphated forms (Fig. 1e).

Composition of perineuronal nets in the visual cortex

We have previously analysed the composition of PNNs in the rat cerebellum and spinal cord. In this study we have characterized PNNs in the visual cortex and found that their composition is the same (Carulli *et al.*, 2006, 2007; Galtrey *et al.*, 2008). The condensed extracellular matrix of PNNs is built around a hyaluronan backbone, to which several types of CSPG and link protein (Crtl1/Hapln1 and Bral2/Hapln4) are bound with tenascin-R binding to the CSPGs, the ensemble forming a dense cartilage-like structure (Carulli *et al.*, 2006, 2007; Dityatev, *et al.*, 2007; Bruckner *et al.*, 2008; Galtrey *et al.*, 2008). In Supplementary Fig. 1, we present a diagram showing a proposed model of the structure of the PNN. In the adult visual cortex we found, as in previous studies, that PNNs are primarily around neurons that express parvalbumin and Kv3.1b, markers of the fast-spiking GABAergic interneurons implicated in ocular dominance control, with 80% of parvalbumin positive neurons being surrounded by PNNs. As in other parts of the CNS, they contain Crtl1, neurocan, aggrecan, phosphacan, brevican and neurocan (Fig. 6 and Supplementary Fig. 2). In mice, PNNs contained Crtl1 and CSPGs and were also predominantly around parvalbumin positive neurons.

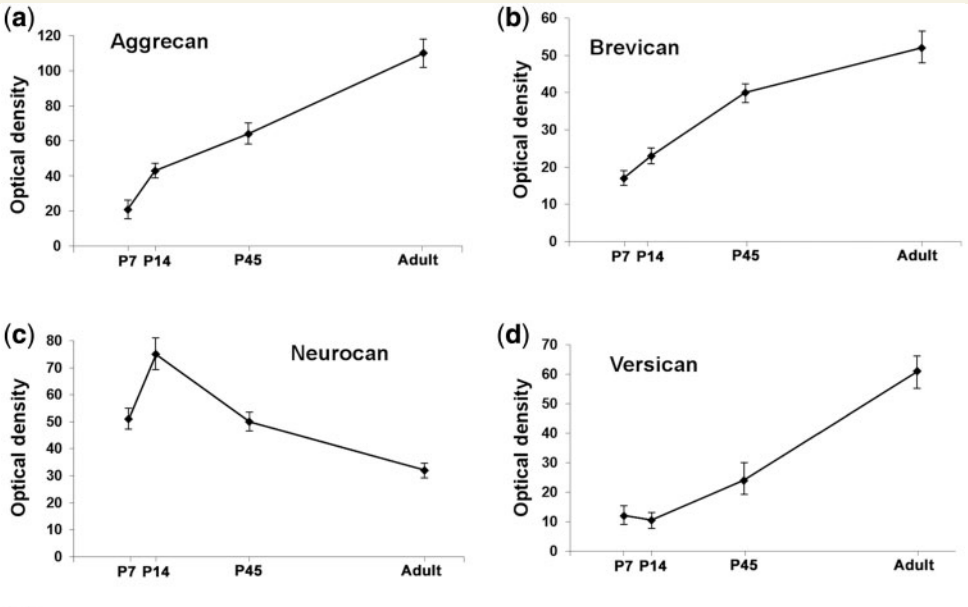

(e)

Disaccharide composition of CS GAG chains in rat cortex during development

Stage	P0	P21	Adult
ΔDi-0S	18.6 (%)	16.0 (%)	3.5 (%)
ΔDi-4S	59.4	59.3	91.5
ΔDi-6S	17.9	12.3	2.5
ΔDi-diS$_D$	1.6	1.2	0.9
ΔDi-diS$_E$	2.5	2.2	1.6

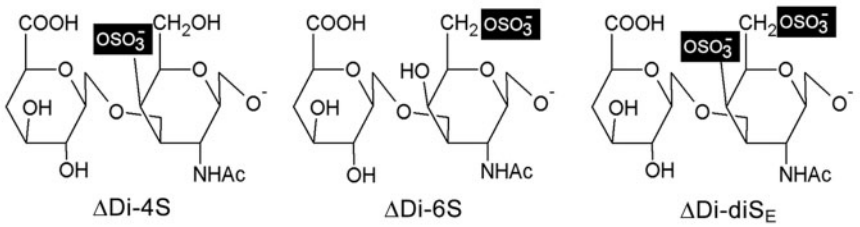

Figure 1 Postnatal changes in CSPGs in the rat posterior cortex. (**a–d**) The levels of four of the major CSPG core proteins change between postnatal Days (P)14 and 45, with increases in aggrecan, brevican and versican, a decrease in neurocan in agreement with previous published reports. (**e**) The sulphation pattern of CSPG glycosaminoglycans (GAGs) at postnatal Days 0, 21 and adulthood in the posterior cortex. For analysis the glycosaminoglycans are digested into disaccharides, three examples of which are shown at the bottom of **e**. The percentage figures in the columns are the percent of total chondroitin sulphate glycosaminoglycan disaccharides that have the sulphation pattern named in the left-hand column. The sulphation pattern changes little between birth and the critical period, after which there is a fall in 6-sulphated and unsulphated glycosaminoglycan and a rise in 4-sulphated glycosaminoglycan. By adulthood 91.5% of glycosaminoglycan is monosulphated at the four position.

Developmental expression of perineuronal net components in visual cortex

Many PNN components are already present in the immature CNS before PNNs form (Carulli *et al.*, 2007; Galtrey *et al.*, 2008). The molecule that triggers construction of the PNNs should be up-regulated as the structures form. This process begins in the rat visual cortex at postnatal Day 14 and at the same age in mice (Fig. 2a–d). We examined the visual cortex during development using *in situ* hybridization and immunohistochemistry to discover which mRNAs and proteins were up-regulated at this time (Fig. 2). Of the mRNAs for PNN components expressed by parvalbumin positive cells, those for hyaluronan synthase, aggrecan, neurocan and tenascin-R were already present by postnatal Day 3, long before PNN formation. Brevican, phosphacan and

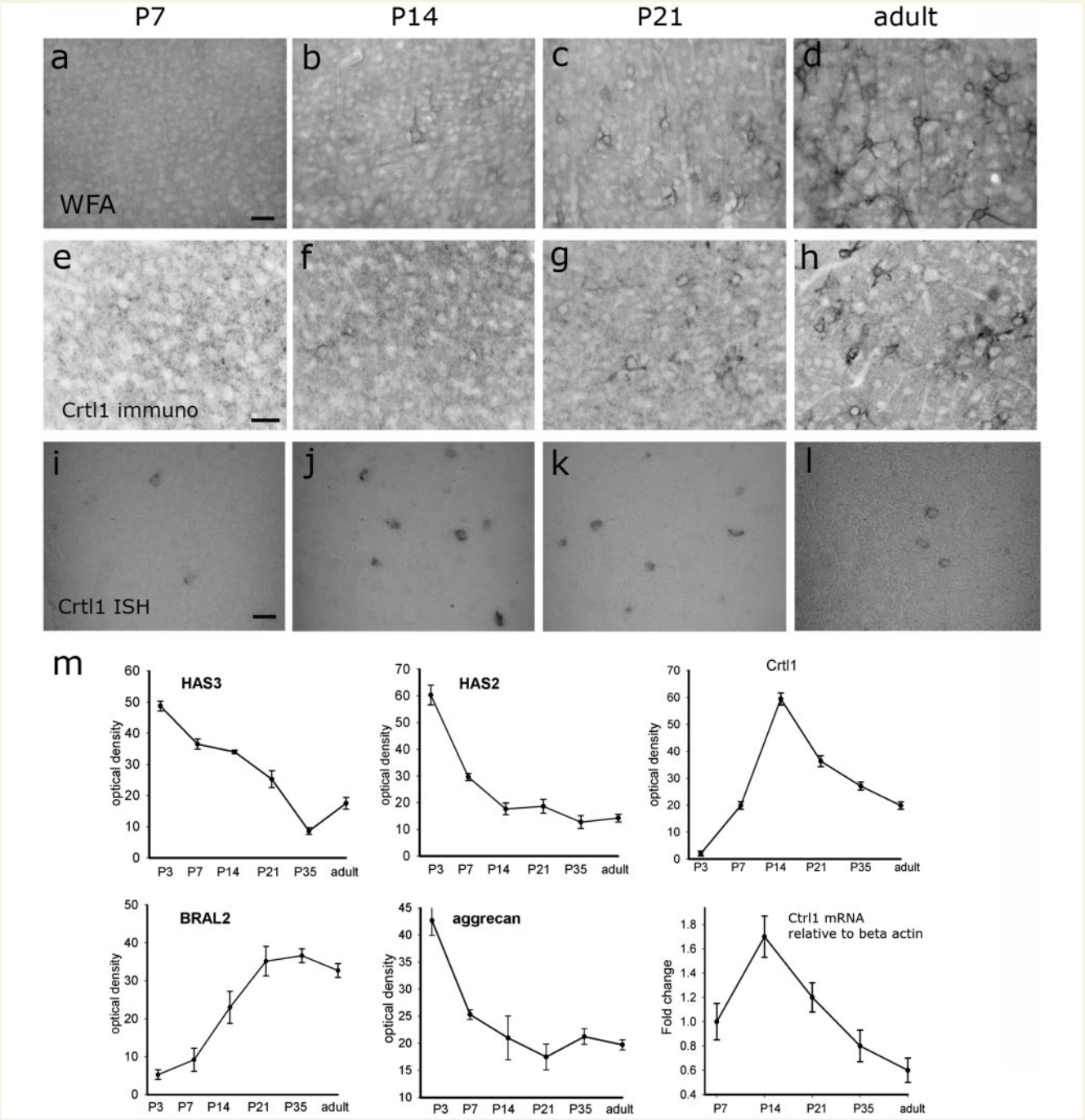

Figure 2 Developmental changes in the expression of PNN components in layers 2/3 of the rat visual cortex. (**a–d**) Staining with *W. floribunda* agglutinin, which reveals most PNNs. The first signs of PNN formation are seen at postnatal Day (P)14. (**e–h**) Immunohistochemistry for link protein Crtl1, showing that it is first detectable from postnatal Day 14, and is present in PNNs. (**i–l**) *In situ* hybridization for Crtl1, showing a peak of neuronal expression as PNNs are forming at postnatal Day 14. (**m**) Quantification of mRNA levels of PNN components by *in situ* hybridization, measuring optical density of selected areas of interest around cortical neurons. The bottom right graph shows Crtl1 mRNA levels in mice measured by quantitative polymerase chain reaction relative to actin, showing that the time course is the same as in rats. HAS = hyaluronan synthase. Bars = 20 μm.

versican, CSPGs that are produced by glial cells, were also present from birth. At postnatal Day 7, before PNN formation, immunohistochemistry showed that all these molecules have a diffuse localization in the visual cortex extracellular matrix, similar to their distribution in the immature spinal cord and cerebellum (Rhodes and Fawcett, 2004; Carulli *et al.*, 2006, 2007; Galtrey *et al.*, 2008). Of the various PNN components, the only two whose mRNAs were up-regulated at the time of PNN formation were the link proteins Crtl1 and Bral2, with Crtl1 showing a peak of expression at postnatal Day 14, coinciding with the onset on PNN

formation, and Bral2 expressed from postnatal Day 21 onwards (Fig. 2e–m). The pattern of Crtl1 expression was the same in mice.

Effects of dark rearing on perineuronal net components in the visual cortex

PNN formation in the visual cortex can be postponed by rearing animals in darkness, and then triggered by light exposure for <1 week (Pizzorusso *et al.*, 2002). As a further step towards identifying the molecules responsible for PNN formation, we asked which PNN components were down-regulated in rats as a result of dark rearing and up-regulated when they were exposed to light. The largest effect of dark rearing on mRNA levels was seen on Ctrl1, where the number of strongly labelled neurons was remarkably reduced (80–90% decrease) in dark reared animals, with the greatest change in cortical layers 2–4 (Fig. 3). On exposure to light, the number of neurons expressing high levels of Crtl1 mRNA reached normal levels after 2 days, at which time the formation of PNNs, visualized with link protein or *W. floribunda* agglutinin staining, was still incomplete (Fig. 3a–h), suggesting that up-regulation of Crtl1 mRNA occurs at the onset of PNN formation. We saw similar but smaller changes in the mRNA levels of Bral2 and hyaluronan synthase 2 in layers 2 and 3, and hyaluronan synthase 3 in layers 5 and 6, all of which showed a 30–40% decrease in the number of labelled neurons after dark rearing

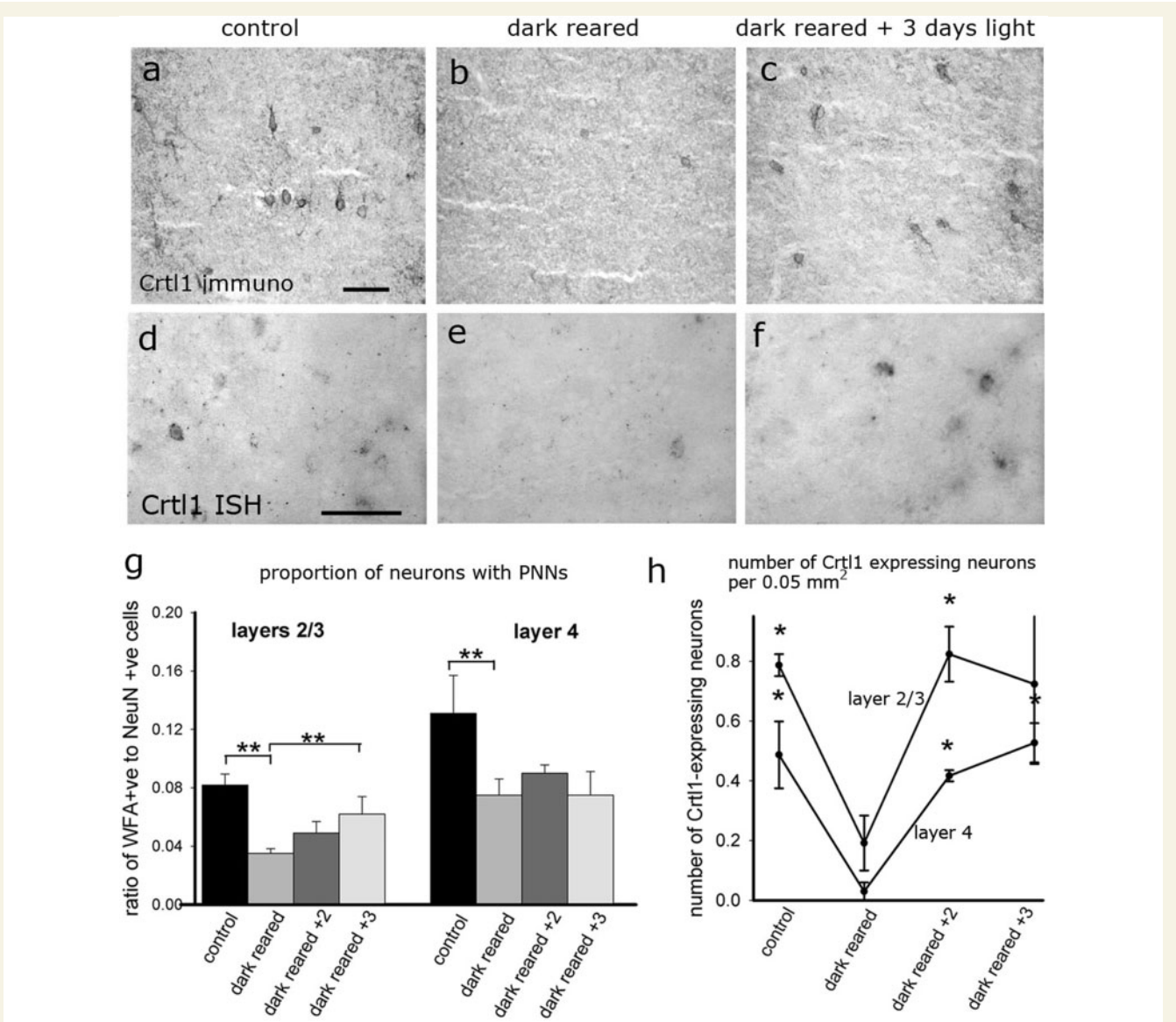

Figure 3 The effects of dark rearing and subsequent light exposure on PNNs and Crtl1 expression in layers 2/3 of the rat visual cortex. (**a–c**) Crtl1 protein in the normal adult cortex (**a**), but much reduced levels after dark rearing (**b**). Three days of exposure to light leads to the beginning of the appearance of Crtl1 in PNNs (**c**). The proportion of neurons with PNNs is quantified in **G** for layers 2/3 and 4. (**d** and **e**) Equivalent pictures of cortical layers 2/3 processed for *in situ* hybridization for Crtl1 mRNA. The mRNA is present in the normal cortex (**d**), down-regulated after dark rearing (**e**) and up-regulated again after light exposure (**f**). These observations are quantified in **h** for cortical layers 2/3 (above) and layer 4 (below). Bars = 50 μm. *$P < 0.05$ relative to control (**g**) and relative to dark reared (**h**).

with a reversion of hyaluronan synthase 2 and hyaluronan synthase 3 to normal levels after 2–3 days of light exposure.

Perineuronal nets in animals lacking Crtl1 in the CNS

The above observations suggest the hypothesis that PNN formation is triggered by the up-regulation of the link protein Crtl1 in parvalbumin positive interneurons. As in cartilage, the link protein might act by stabilizing the binding of the various CSPGs to hyaluronan (Morgelin *et al.*, 1994; Watanabe *et al.*, 1998). Hyaluronan is present around neurons that have PNNs because they all express hyaluronan synthase from an early stage (Carulli *et al.*, 2006, 2007; Galtrey *et al.*, 2008). The presence of link protein could therefore allow the capture of CSPGs into the hyaluronan pericellular coat around parvalbumin neurons. In order to test this hypothesis we produced transgenic mice lacking Crtl1 in the adult CNS. Previous work has generated animals completely lacking Crtl1; these die at birth because they are unable to form hyaline cartilage, therefore lacking the cartilaginous rings that keep the trachea and bronchi patent, and they also have cardiac defects. We therefore generated rescue transgenic mice in which the natural *Crtl1* gene was knocked out and replaced with a transgene expressed under the control of the type II collagen cartilage-specific promoter and enhancer (Czipri *et al.*, 2003). Crtl1 protein was not detectable in the brain of adult transgenics (Supplementary Fig. 3). The animals showed no obvious behavioural abnormality, were able to feed and reproduce normally and showed no signs of reduced cortical inhibition such as a tendency to fits. Immunohistochemistry for the PNN markers aggrecan and *W. floribunda* agglutinin, for several CSPGs and with hyaluronan binding protein, showed that PNNs in the Crtl1 knockout animals were very attenuated (Fig. 4). In normal cortex, PNNs surround the neuronal soma and dendrites, but in knockout animals *W. floribunda* agglutinin and aggrecan staining around the dendrites was absent, although there was some attenuated staining around the somata. The appearance is different to the partly-formed PNNs that form in the absence of tenascin-R (Bruckner *et al.*, 2000). Quantification of *W. floribunda* agglutinin staining in knockout animals, including the attenuated PNNs in the counts, showed a 25% reduction in the proportion of parvalbumin positive neurons with PNNs (Fig. 5). The main change was a large reduction in the area of the *W. floribunda* agglutinin positive profiles due to the absence of staining around dendrites, and in the intensity of *W. floribunda* agglutinin staining around parvalbumin positive neurons (Figs 4g–h and 5). The overall number, size and number of processes of parvalbumin positive neurons was unchanged (Fig. 5). We saw similar changes around the neurons of the cuneate nucleus (Fig. 4 i,j).

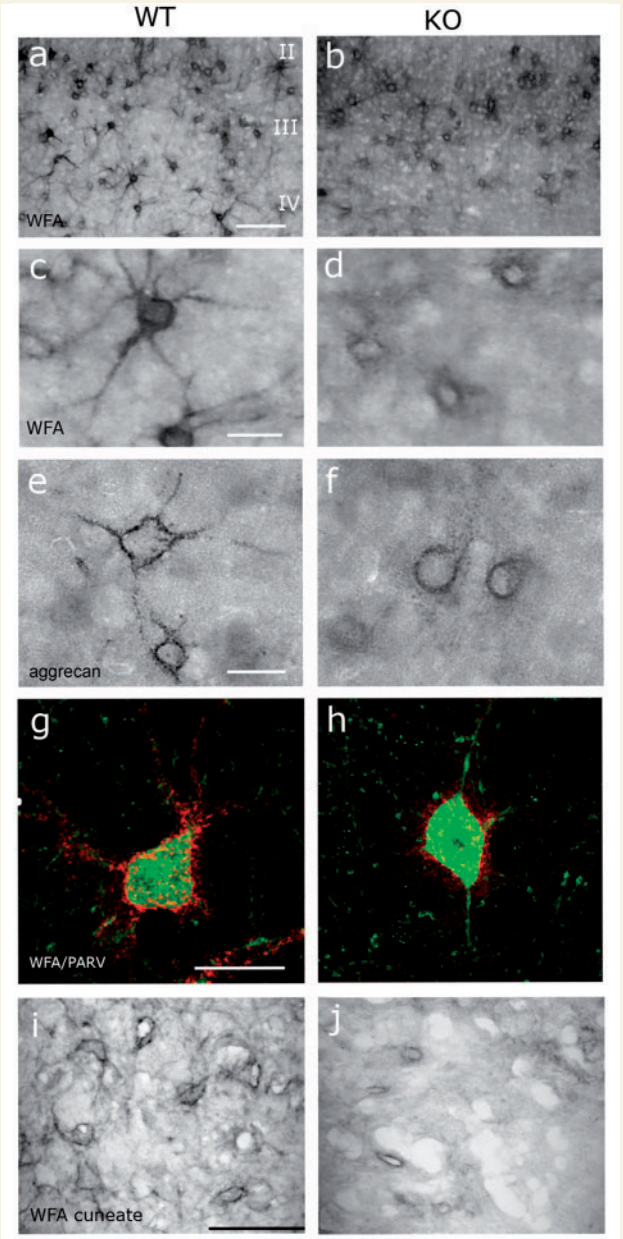

Figure 4 The appearance of PNNs in wild-type and Crtl1 knockout animals. (**a–d**) *W. floribunda* agglutinin staining of the visual cortex layer 3, comparing PNNs at low and high power and showing the absence of PNN around dendrites in Crtl1 knockouts. A similar appearance is seen with aggrecan staining (**e** and **f**). The absence of PNNs around parvalbumin-positive neuron dendrites in knockouts is not due to the absence of dendrites in knockout animals; (**g** and **h**) parvalbumin stained neurons in normal and knockout animals with normal dendritic morphology, but with less *W. floribunda* agglutinin-stained PNN in knockout animals (**h**). (**i** and **j**) *W. floribunda* agglutinin staining of the cuneate nucleus in normal and knockout animals. Bars = 70 μm (**a** and **b**); 15 m (**c–h**); 50 m (**i** and **j**).

CSPG and NogoR levels in Crtl1 knockout animals

In Crtl1 knockout animals we examined the protein levels and distribution of aggrecan, phosphacan, neurocan-N, brevican, versican, tenascin-R and the distribution of hyaluronan in the visual cortex by western blot and immunohistochemistry (Fig. 6). All of these molecules were present in the cortex in the same quantity as in normal animals, except for neurocan-N which was

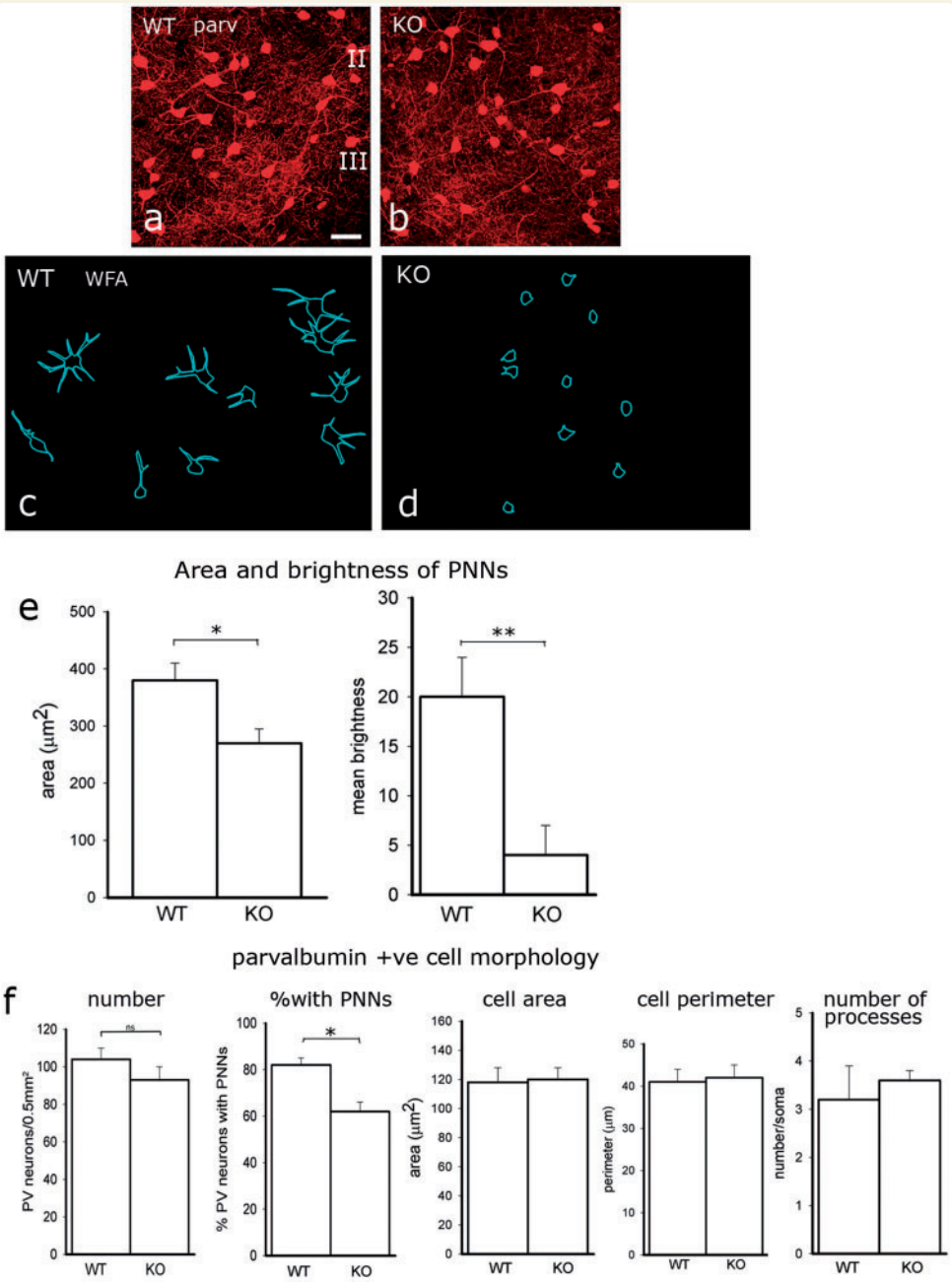

Figure 5 Quantification of the anatomy of parvalbumin-positive neurons. A low-power picture of parvalbumin (PV) staining (**a** and **b**) shows no gross difference between control and Crtl1 knockout animals. To measure the size of *W. floribunda* agglutinin positive PNNs, a perimeter was drawn around the stained regions of neurons and the areas of the tracings measured (**c** and **d**). The size and *W. floribunda* agglutinin staining intensity of the PNNs is shown in **e**. Slightly fewer of the neurons are surrounded by PNNs in the Crtl1 knockouts, and the PNNs in the knockouts are attenuated in size and staining intensity (**e** and **f**). The number and anatomy of the parvalbumin positive neurons is normal in the Crtl1 knockout animals (**f**). Bar = 40 μm. WT = wild-type; KO = knockout. $*P < 0.05$; $**P < 0.001$.

30% reduced. The molecules were, however, diffusely spread and not condensed into PNNs, although some aggrecan, hyaluronan and tenascin-R were present in the attenuated PNNs around the somata. The more stable components of the extracellular matrix can only be extracted in 6 M urea, and some PNN components, particularly neurocan-N and versican, are preferentially represented in this compartment (Deepa *et al.*, 2006). In Crtl1 knockout brains, neurocan-N was absent from the 6 M urea fraction, but a stable urea-extractible extracellular matrix compartment persisted, which contained normal amounts of the other CSPGs. These findings demonstrate that the overall levels of matrix components are not changed in the Crtl1 knockout animals. The lack of fully formed PNNs in the Crtl1 CNS-knockout is therefore not due to the absence of the other PNN components,

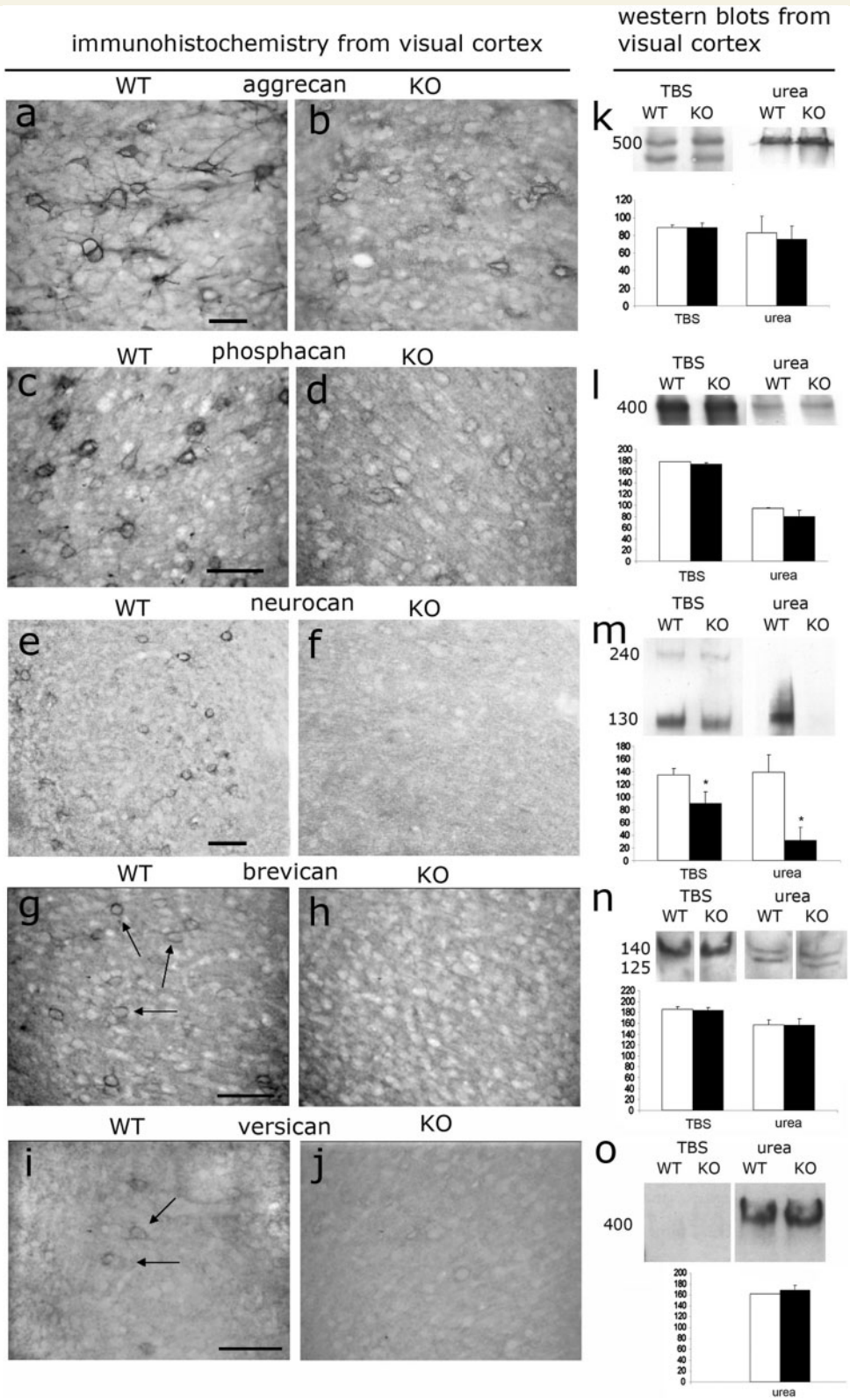

Figure 6 The lack of link protein affects the distribution but not the overall quantity of several CSPGs that are normally enriched in PNNs. The pictures show layers 2/3 of visual cortex. In control (WT) animals, the PNNs contain the same CSPGs as in rats (**a**,**c**,**e**,**g**,**i**). In Crtl1 knockout animals vestigial PNNs are still seen, with attenuated aggrecan and phosphacan staining localized just around the cell soma (**b**,**d**). Neurocan staining is barely visible (**f**), and brevican and versican staining are absent (**h**,**j**). However there is diffuse staining for all the CSPGs in knockouts. The western blots from cortical tissue (**k**,**l**,**m**,**n**,**o**) show that all the CSPGs are present in the brains of Crtl1 knockouts in normal overall amounts, except for neurocan-N, which is 30% decreased in the Tris buffered saline (TBS) extract and is no longer seen in the stable matrix compartment that can only be extracted in 6 M urea. The protein quantifications are taken from three independent western blots. Bars = 30 μm. WT = wild-type; KO = knockout.

but rather to the absence of the structure that stabilizes them as PNNs around the cell bodies and dendrites of parvalbumin positive interneurons. In addition, we examined the levels of Nogo receptor in normal and Crtl1 knockout animals because these molecules also affect ocular dominance plasticity (McGee *et al.,* 2005). We found no differences (Supplementary Fig. 4).

Ocular dominance plasticity in animals lacking *Crtl1* in the CNS

We then investigated whether ocular dominance plasticity persists into adulthood in the Crtl1 CNS-knockout animals. Even normal mice show some ocular dominance plasticity in early adulthood if monocular deprivation persists for more than 3 days (Sawtell *et al.,* 2003; Sato and Stryker, 2008). We therefore submitted animals that were at least 13 weeks in age to only 3 days of monocular deprivation, after which ocular dominance was examined by electrophysiological recordings of visual evoked potentials. Visual evoked potentials represent the integrated response of a population of neurons to patterned visual stimuli and this is mainly due to subthreshold responses. Responsiveness of the mouse visual cortex to stimulation of the eye has been measured using a number of methods, including single-unit recordings, visual evoked potentials, optical imaging of intrinsic signals, immediate early gene expression and two-photon imaging of cellular calcium transients. Although each method is related to specific aspects of neuronal response, all methods yield a consistent picture of what happens after an eye is deprived (Smith *et al.,* 2009). We used visual evoked potentials because they make it possible to compare the response strength to each eye and, by increasing stimulus spatial frequency, it is possible to assess the spatial resolution threshold of each eye. Monocular deprivation during the sensitive period affects both response amplitude and visual acuity (for review, see Morishita and Hensch, 2008), and both of these can be assessed using visual evoked potential recordings. We show typical visual evoked potential recordings at different cortical depths in Fig. 7a.

In normal animals, no change in the amplitude ratio between the contralateral and the ipsilateral eye (*C/I* ratio) was seen after monocular deprivation, but in animals lacking Crtl1 there was a shift of the *C/I* ratio towards the ipsilateral non-deprived eye of similar magnitude to that seen during the critical period (Fig. 7b). Visual evoked potential visual acuity correlates well with behavioural estimates of visual acuity, so we also asked whether monocular deprivation affected visual evoked potential visual acuity in adult Crtl1 knockout mice. Non-deprived Crtl1 knockout mice had a normal visual evoked potential ratio, visual acuity and visual evoked potential amplitude curve (Fig. 7c and d).

This result excludes general abnormalities in excitatory/inhibitory balance controlling neuronal activity and visual responses in these mice. Crtl1 knockout mice monocularly deprived for 3 days showed a considerable decrease in visual acuity that dropped to ~0.3 c/deg (Fig. 7c). In addition, visual evoked potential amplitude in response to visual stimulation of the deprived contralateral eye indicated that deprived eye visual evoked potential responses to stimuli of high spatial frequency (0.2 and 0.3 c/deg) (Fig. 7c) were also affected in Crtl1 knockout but not in wild-type mice. Thus, adult Crtl1 mice with disrupted PNNs display levels of plasticity capable of shifting the balance of the *C/I* ratio and reducing visual acuity of the deprived eye, a behaviourally relevant property of vision. We were able to observe overall levels of electrical activity in the groups of animals. The Crtl1 knockout animals had the same level of spontaneous cortical activity as control animals, suggesting that there is no loss of cortical inhibition.

Plasticity in the cuneate nucleus in Crtl1 knockout animals

ChABC treatment has been shown to promote anatomical sprouting of axons into denervated regions (Massey *et al.,* 2006; Cafferty *et al.,* 2008; Garcia-Alias *et al.,* 2009; Tom *et al.,* 2009). We wished to see whether the absence of PNNs might have a similar effect. We therefore used the experimental model developed by Massey *et al.* (2008), in which sprouting of preserved ascending sensory axons into denervated regions of the cuneate nucleus was promoted by ChABC. We performed unilateral dorsal hemisection lesions of the spinal cord of control and Crtl1 knockout mice between levels C6 and C7. This lesion cuts ascending sensory axons from the medial two digits of the forepaws but leaves those from the lateral digits intact. One week after injury we injected cholera toxin B subunit into the forepaw of animals, labelling ascending sensory axons by transganglionic transport. In control animals sensory axon innervation of the cuneate nucleus was restricted to the region normally innervated by the lateral digits with no apparent sprouting into the denervated regions. In Crtl1 knockout animals, we saw labelled axons innervating the regions previously innervated by the medial digits, indicating sprouting of the preserved axons (Fig. 8a–c). Quantification of this sprouting by drawing a perimeter around all the labelled axons showed a significantly larger area occupied by axons from the Crtl1 knockout animals (Fig. 8d).

Discussion

The experiments in this article were designed to identify the developmental changes in the extracellular matrix that modulate the ability of the CNS to undergo plastic change and therefore the probable target through which ChABC reactivates plasticity and promotes recovery of function. We demonstrate that there are several changes in the extracellular matrix during the critical period with changes in core protein levels, glycosaminoglycan sulphation patterns and the onset of PNN formation. The main hypothesis we have tested is that the PNNs are responsible for limiting plasticity in the adult CNS. Our results support this idea; we have shown that the triggering of PNN formation by the production of link protein is the major event in the extracellular matrix that limits plasticity in both the visual cortex and the cuneate nucleus. This event must act with Nogo and other factors associated with parvalbumin positive interneurons to control plasticity in the cortex (Hensch, 2005; McGee *et al.,* 2005; Hofer *et al.,* 2006; Tropea *et al.,* 2008; Datwani *et al.,* 2009).

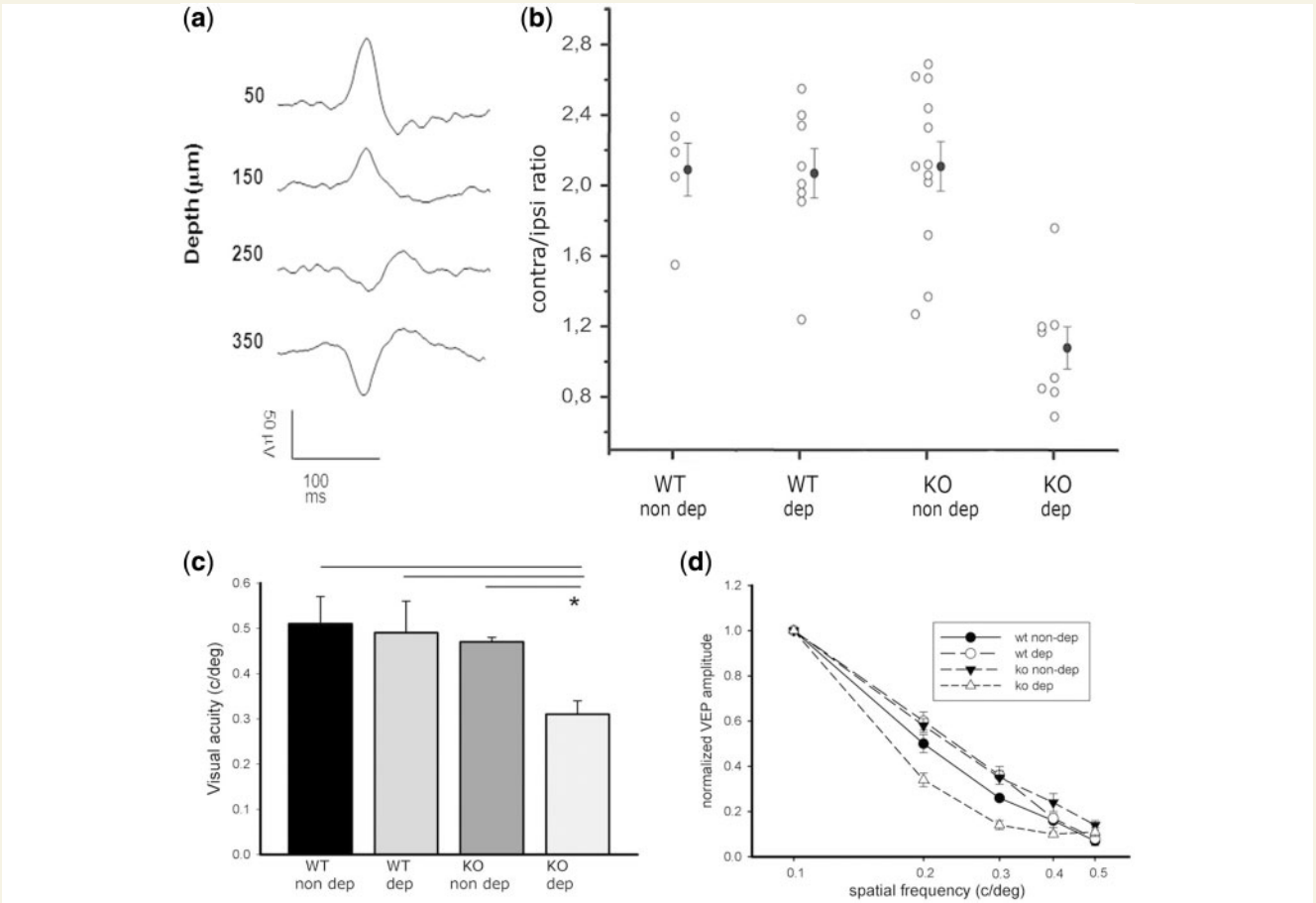

Figure 7 Ocular dominance plasticity in adult Crtl1 knockout mice. (**a**) A typical set of visual evoked potential recordings, with a reversal of polarity with increasing depth in the visual cortex. (**b**) Visual evoked potential *C/I* ratio in wild-type (WT) and Crtl1 knockout (KO) littermates. Each circle represents a single animal. Normal and knockout animals have the usual *C/I* ratio of visual evoked potential response amplitude of 2.2. After 3 days of monocular deprivation (dep) control animals show no ocular dominance shift, but Crtl1 knockouts show an ocular dominance shift to near unity, similar to that seen in animals during the critical period (two way ANOVA, *post hoc* Tukey's test, $*P<0.05$). (**c**) Crtl1 knockout deprived for 3 days show a decrease in visual acuity. In addition, the visual evoked potential amplitude versus spatial frequency curve (**d**) of the deprived contralateral eye indicates that visual evoked potential amplitude is affected not only at the low spatial frequency (0.1 c/deg) stimulus used for the *C/I* ratio, but also at stimuli of higher spatial frequency (0.2 and 0.3 c/deg). Non-deprived Crtl1 mice have normal visual acuity and visual evoked potential curves, excluding general abnormalities in the visual properties of these mice (two way ANOVA, *post hoc* Tukey's test, $*P<0.05$). The dashed line in **c** represents noise level.

The composition of the extracellular matrix in the CNS is similar to that of other parts of the body, except for the absence of fibrillar collagen. In previous experiments we analysed the composition of the two extracellular matrix compartments of the CNS, the diffuse extracellular matrix that is found throughout the CNS and the condensed matrix of the PNNs that are found around neurons. Both types of extracellular matrix contain several CSPGs together with long chains of hyaluronan, tenascin-C and tenascin-R. The condensed extracellular matrix of PNNs contains these molecules with the addition of one or more link proteins (Crtl1/Hapln1 and Bral2/Hapln4) and larger amounts of tenascin-R, the ensemble forming a dense cartilage-like structure (Carulli *et al.,* 2006, 2007; Deepa *et al.,* 2006; Dityatev *et al.,* 2007; Bruckner *et al.,* 2008; Galtrey *et al.,* 2008). Some of the molecules found in PNNs (hyaluronan synthase, aggrecan, neurocan, link protein) are produced by the neurons, the others by surrounding glia (Carulli *et al.,* 2006, 2007). Which of the molecules produced by PNN-enveloped neurons triggers their formation? One way to answer the question is to determine which molecule is up-regulated just as PNNs start to form. Our observations show that of the many molecules comprising PNNs, only link protein Crtl1 starts to be expressed at this moment in development, with aggrecan expression starting earlier and the other components being present much earlier during embryogenesis. PNN formation can be delayed then triggered by dark rearing followed by exposure to light (Pizzorusso *et al.,* 2002) and again, Crtl1 expression closely followed the time course of PNN formation.

In order to test the hypothesis that Crtl1 expression is the trigger for PNN formation, we examined mice that lack Crtl1 in the adult CNS. Previous work had generated animals completely lacking Crtl1; these died at birth because they are unable to form hyaline cartilage and also had cardiac defects. We therefore

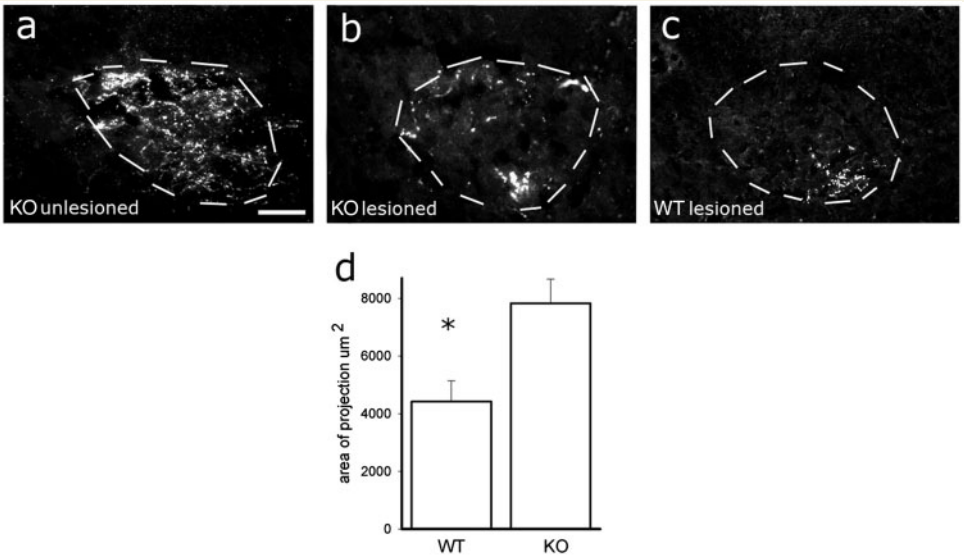

Figure 8 Cholera toxin B injections into the forepaw label sensory axons occupying the entire cross-section of the cuneate nucleus. Axons traced from the forepaw are shown in a knockout (KO) animal, with the outer extent of the nucleus traced (**a**). The appearance is the same in wild-type (WT) mice. After a dorsal column hemisection lesion between C6 and C7, innervation of the cuneate nucleus from the forepaw is reduced to the area occupied by the two lateral digits. In Crtl1 knockout (**b**) $n = 7$, but not in control animals (**c**) $n = 12$. These unlesioned connections sprout to re-innervate the regions normally innervated by the medial two digits. (**d**) Quantification of this sprouting was performed by tracing around the outline of the stained terminals then measuring the area of innervation ($^*P < 0.05$ by *t*-test). Bar = 100 μm.

generated rescue transgenic mice in which Crtl1 was expressed under the control of the type II collagen cartilage-specific promoter and enhancer, leading to Crtl1 expression in cartilage but not in the adult CNS (Czipri *et al.,* 2003). In the visual cortex and elsewhere in the CNS these animals had attenuated PNNs, with no PNN material around dendrites and vestigial PNNs surrounding the cell somata; we suggest that this residual PNN formation is due to the production of aggrecan by the neurons. There is abundant evidence that PNN formation is modulated by electrical activity, behavioural experience, brain-derived neurotrophic factor and insulin-like growth factors. Our results suggest that these influences must have effects on Crtl1 expression (Kalb and Hochfield, 1994; Berghuis *et al.,* 2004; Miyata *et al.,* 2004; Ciucci *et al.,* 2007; Dityatev *et al.* 2007; Reimers *et al.,* 2007).

Because Crtl1 knockout animals have only vestigial PNNs we were able to ask whether animals lacking PNNs showed continuing plasticity into adulthood. First, we asked whether the absence of Crtl1 led to changes in the overall levels of the CSPG core proteins or in the pattern of sulphation of their glycosaminoglycan chains. We found no significant change from wild-type littermate mice in glycosaminoglycan sulphation or in the overall levels of the CSPG core proteins, the difference is that CSPGs are diffusely spread rather than concentrated in PNNs. There was also no change in the level of the Nogo receptor, which has been shown to affect ocular dominance plasticity (McGee *et al.*, 2005). The only significant difference between the extracellular matrix of Crtl1 knockout and control mice was the absence of PNNs. We could therefore ask whether the absence of PNNs has an effect on plasticity. We used two models in which treatment with ChABC has been shown to reactivate plasticity in the adult CNS. Ocular dominance plasticity is much diminished in mice after postnatal Day 35, and in adult animals such as we used, 3 days of monocular deprivation has no effect on either ocular dominance or on visual acuity (Sawtell *et al.*, 2003; Sato and Stryker, 2008). However in Crtl1 knockout animals, 3 days of monocular deprivation led to a shift in ocular dominance and a loss of visual acuity similar in magnitude to that seen during the critical period. We also examined anatomical plasticity in another model in which terminal sprouting into denervated territory is enhanced by ChABC treatment (Massey *et al.*, 2006). Transection of the dorsal columns at spinal levels C6–7 cuts sensory axons connecting the two medial digits to the cuneate nucleus but leaves connections from the lateral digits intact. In previous work there was no growth of the preserved terminals into the denervated regions, but after treatment with ChABC, the residual sensory inputs sprouted into the denervated regions. The Crtl1 knockout responded to partial denervation of the cuneate nucleus similarly to ChABC treated animals with sprouting of the residual axons into denervated regions of the cuneate nucleus, but this did not occur in control animals.

Our observations suggest that in adult animals, the presence of PNNs is the key factor in the extracellular matrix-related restriction of plasticity. Evidence for this also comes from animals lacking tenascin-R, which have abnormal PNNs and retain some plasticity in adulthood (Apostolova *et al.,* 2006). However, glycosaminoglycan sulphation may also play a part since we found that adult animals lacking the enzyme for 6-sulphation of glycosaminoglycan were less plastic then normal (Lin *et al*., unpublished results). The way in which PNNs might restrict plasticity is not known. PNNs contain CSPGs and tenascin, both of which are inhibitory to

neurite growth, and both of which may prohibit the formation of new connections on dendrites. The perineuronal extracellular matrix also influences glutamate receptor mobility (Frischknecht *et al.,* 2009). Within the adult CNS, members of the semaphorin3 family are widely expressed, but Sema3A protein binds preferentially to PNN glycans, leading to localization of Sema3A on PNNs (Vo *et al.,* 2007). Sema3A, through its effects on synapse dynamics, could be a mediator of the effects of PNNs on plasticity (Bouzioukh *et al.,* 2006). Overall, therefore, the PNN might act as a barrier to ingrowth of new connections and might also restrict dendritic plasticity and sprouting, which would also have the effect of preventing the formation of new connections. PNNs also attract the homeobox protein Otx2 to parvalbumin positive interneurons affecting their maturation and physiological properties (Sugiyama *et al.,* 2008). CSPGs in PNNs have different binding properties to those in the diffuse CNS matrix (Deepa *et al.,* 2006), but their binding is nevertheless fairly promiscuous. They probably attract a number of active molecules around the parvalbumin positive interneurons, which affect their function. The effect of PNNs on plasticity is probably different to that of anti-NogoA or neurotrophins, whose main action is to promote axonal sprouting.

Overall, our findings demonstrate that the formation of PNNs triggered by neuronal Crtl1 synthesis is a key event in the diminuation of plasticity in the adult CNS and suggest that modification of PNNs is how CSPGs reactivate plasticity. Understanding how PNNs form and how they exert their effects should make it possible to identify a new range of therapeutic possibilities for the modulation of CNS plasticity and functional recovery after CNS damage.

Funding

This work was supported by grants from the Medical Research Council, the Wellcome Trust, The Christopher and Dana Reeve Foundation, The European Union Framework 6 Network of Excellence NeuroNE, The European Union Framework 7 Projects Plasticise and Eurov1sion, The Henry Smith Charity, The John and Lucille van Geest foundation, the Italian Ministry for University and Research and the IIT seed project Extraplast.

Conflict of interest: J.F. is a paid consultant for Acorda Therapeutics, which is involved in the commercial development of chondroitinase.

Supplementary material

Supplementary material is available at *Brain* online.

References

Apostolova I, Irintchev A, Schachner M. Tenascin-R restricts posttraumatic remodeling of motoneuron innervation and functional recovery after spinal cord injury in adult mice. J Neurosci 2006; 26: 7849–59.

Balmer TS, Carels VM, Frisch JL, Nick TA. Modulation of perineuronal nets and parvalbumin with developmental song learning. J Neurosci 2009; 29: 12878–85.

Barritt AW, Davies M, Marchand F, Hartley R, Grist J, Yip P, et al. Chondroitinase ABC promotes sprouting of intact and injured spinal systems after spinal cord injury. J Neurosci 2006; 26: 10856–67.

Berghuis P, Dobszay MB, Sousa KM, Schulte G, Mager PP, Hartig W, et al. Brain-derived neurotrophic factor controls functional differentiation and microcircuit formation of selectively isolated fast-spiking GABAergic interneurons. Eur J Neurosci 2004; 20: 1290–306.

Blakemore C, Van Sluyters RC. Reversal of the physiological effects of monocular deprivation in kittens: further evidence for a sensitive period. J Physiol 1974; 237: 195–216.

Bouzioukh F, Daoudal G, Falk J, Debanne D, Rougon G, Castellani V. Semaphorin3A regulates synaptic function of differentiated hippocampal neurons. Eur J Neurosci 2006; 23: 2247–54.

Bruckner G, Grosche J, Schmidt S, Hartig H, Margolis RU, Delpech B, et al. Post-natal development of perineuronal nets in wild-type mice and in a mutant deficient in tenascin-R. J Comp Neurol 2000; 428: 616–29.

Bruckner G, Morawski M, Arendt T. Aggrecan-based extracellular matrix is an integral part of the human basal ganglia circuit. Neuroscience 2008; 151: 489–504.

Busch SA, Silver J. The role of extracellular matrix in CNS regeneration. Curr Opin Neurobiol 2007; 17: 120–7.

Cafferty WB, Bradbury EJ, Lidierth M, Jones M, Duffy PJ, Pezet S, et al. Chondroitinase ABC-mediated plasticity of spinal sensory function. J Neurosci 2008; 28: 11998–2009.

Calabro A, Midura R, Wang A, West L, Plaas A, Hascall VC. Fluorophore-assisted carbohydrate electrophoresis (FACE) of glycosaminoglycans. Osteoarthritis Cartilage 2001; 9(Suppl A): S16–S22.

Carulli D, Deepa SS, Fawcett JW. Upregulation of aggrecan, link protein 1 and hyaluronan synthases during formation of perineuronal nets in the rat cerebellum. J Comp Neurol 2007; 501: 83–94.

Carulli D, Rhodes KE, Brown DJ, Bonnert TP, Pollack SJ, Oliver K, et al. The composition of perineuronal nets in the adult rat cerebellum and the cellular origin of their components. J Comp Neurol 2006; 494: 559–77.

Ciucci F, Putignano E, Baroncelli L, Landi S, Berardi N, Maffei L. Insulin-like growth factor 1 (IGF-1) mediates the effects of enriched environment (EE) on visual cortical development. PLoS ONE 2007; 2: e475.

Curinga GM, Snow DM, Mashburn C, Kohler K, Thobaben R, Caggiano AO, et al. Mammalian-produced chondroitinase AC mitigates axon inhibition by chondroitin sulfate proteoglycans. J Neurochem 2007; 102: 275–88.

Czipri M, Otto JM, Cs-Szabo G, Kamath RV, Vermes C, Firneisz G, et al. Genetic rescue of chondrodysplasia and the perinatal lethal effect of cartilage link protein deficiency. J Biol Chem 2003; 278: 39214–223.

Datwani A, McConnell MJ, Kanold PO, Micheva KD, Busse B, Shamloo M, et al. Classical MHCI molecules regulate retinogeniculate refinement and limit ocular dominance plasticity. Neuron 2009; 64: 463–70.

Deepa SS, Carulli D, Galtrey C, Rhodes K, Fukuda J, Mikami T, et al. Composition of perineuronal net extracellular matrix in rat brain: a different disaccharide composition for the net-associated proteoglycans. J Biol Chem 2006; 281: 17789–800.

Dityatev A, Bruckner G, Dityateva G, Grosche J, Kleene R, Schachner M. Activity-dependent formation and functions of chondroitin sulfate-rich extracellular matrix of perineuronal nets. Dev Neurobiol 2007; 67: 570–88.

Fagiolini M, Fritschy JM, Low K, Mohler H, Rudolph U, Hensch TK. Specific GABAA circuits for visual cortical plasticity. Science 2004; 303: 1681–3.

Fawcett JW, Curt A. Damage control in the nervous system: rehabilitation in a plastic environment. Nat Med 2009; 15: 735–6.

Frischknecht R, Heine M, Perrais D, Seidenbecher CI, Choquet D, Gundelfinger ED. Brain extracellular matrix affects AMPA receptor lateral mobility and short-term synaptic plasticity. Nat Neurosci 2009; 12: 897–904.

Galtrey CM, Asher RA, Nothias F, Fawcett JW. Promoting plasticity in the spinal cord with chondroitinase improves functional recoveryafter peripheral nerve repair. Brain 2007; 130: 926–39.

Galtrey CM, Kwok JC, Carulli D, Rhodes KE, Fawcett JW. Distribution and synthesis of extracellular matrix proteoglycans, hyaluronan, link proteins and tenascin-R in the rat spinal cord. Eur J Neurosci 2008; 27: 1373–90.

Garcia-Alias G, Barkhuysen S, Buckle M, Fawcett JW. Chondroitinase ABC treatment opens a window of opportunity for task-specific rehabilitation. Nat Neurosci 2009; 12: 1145–51.

Girgis J, Merrett D, Kirkland S, Metz GA, Verge V, Fouad K. Reaching training in rats with spinal cord injury promotes plasticity and task specific recovery. Brain 2007; 130: 2993–3003.

Gogolla N, Caroni P, Luthi A, Herry C. Perineuronal nets protect fear memories from erasure. Science 2009; 325: 1258–61.

Gordon JA, Stryker MP. Experience-dependent plasticity of binocular responses in the primary visual cortex of the mouse. J Neurosci 1996; 16: 3274–86.

Harauzov A, Spolidoro M, DiCristo G, De Pasquale R, Cancedda L, Pizzorusso T, et al. Reducing intracortical inhibition in the adult visual cortex promotes ocular dominance plasticity. J Neurosci 2010; 30: 361–71.

Hensch TK. Critical period plasticity in local cortical circuits. Nat Rev Neurosci 2005; 6: 877–88.

Hockfield S, Kalb RG, Zaremba S, Fryer H. Expression of neural proteoglycans correlates wityh the acquisition of mature neuronal properties in the mammalian brain. Cold Spring Harbor Symp Quant Biol 1990; 55: 505–13.

Hofer SB, Mrsic-Flogel TD, Bonhoeffer T, Hubener M. Lifelong learning: ocular dominance plasticity in mouse visual cortex. Curr Opin Neurobiol 2006; 16: 451–9.

Houle JD, Amin A, Cote MP, Lemay M, Miller K, Sandrow H, et al. Combining peripheral nerve grafting and matrix modulation to repair the injured rat spinal cord. J Vis Exp 2009Advance Access published on November 20, 2009, doi: 10.3791/1324.

Iaci JF, Vecchione AM, Zimber MP, Caggiano AO. Chondroitin sulfate proteoglycans in spinal cord contusion injury and the effects of chondroitinase treatment. J Neurotrauma 2007; 24: 1743–59.

Kalb RG, Hockfield S. Electrical activity in the neuromuscular unit can influence the molecular development of motor neurons. Dev Biol 1994; 162: 539–48.

Kitagawa H, Tsutsumi K, Tone Y, Sugahara K. Developmental regulation of the sulfation profile of chondroitin sulfate chains in the chicken embryo brain. J Biol Chem 1997; 272: 31377–81.

Kwok JC, Afshari F, Garcia-Alias G, Fawcett JW. Proteoglycans in the central nervous system: plasticity, regeneration and their stimulation with chondroitinase ABC. Restor Neurol Neurosci 2008; 26: 131–45.

Lehmann K, Lowel S. Age-dependent ocular dominance plasticity in adult mice. PLoS ONE 2008; 3: e3120.

Massey JM, Amps J, Viapiano MS, Matthews RT, Wagoner MR, Whitaker CM, et al. Increased chondroitin sulfate proteoglycan expression in denervated brainstem targets following spinal cord injury creates a barrier to axonal regeneration overcome by chondroitinase ABC and neurotrophin-3. Exp Neurol 2008; 209: 426–45.

Massey JM, Hubscher CH, Wagoner MR, Decker JA, Amps J, Silver J, et al. Chondroitinase ABC digestion of the perineuronal net promotes functional collateral sprouting in the cuneate nucleus after cervical spinal cord injury. J Neurosci 2006; 26: 4406–14.

McGee AW, Yang Y, Fischer QS, Daw NW, Strittmatter SM. Experience-driven plasticity of visual cortex limited by myelin and Nogo receptor. Science 2005; 309: 2222–6.

McRae PA, Rocco MM, Kelly G, Brumberg JC, Matthews RT. Sensory deprivation alters aggrecan and perineuronal net expression in the mouse barrel cortex. J Neurosci 2007; 27: 5405–13.

Milev P, Maurel P, Chiba A, Mevissen M, Popp S, Yamaguchi Y, et al. Differential regulation of expression of hyaluronana-binding proteoglycans in develoiping brain: aggrecan, versican, neurocan and brevican. Biochem Biophys Res Commun 1998; 247: 207–12.

Miyata S, Akagi A, Hayashi N, Watanabe K, Oohira A. Activity-dependent regulation of a chondroitin sulfate proteoglycan 6B4 phosphacan/RPTPbeta in the hypothalamic supraoptic nucleus. Brain Res 2004; 1017: 163–71.

Morgelin M, Heinegard D, Engel J, Paulsson M. The cartilage proteoglycan aggregate: assembly through combined protein-carbohydrate and protein-protein interactions. Biophys Chem 1994; 50: 113–28.

Morishita H, Hensch TK. Critical period revisited: impact on vision. Curr Opin Neurobiol 2008; 18: 101–7.

Nakamura M, Nakano K, Morita S, Nakashima T, Oohira A, Miyata S. Expression of chondroitin sulfate proteoglycans in barrel field of mouse and rat somatosensory cortex. Brain Res 2009; 1252: 117–29.

Pizzorusso T, Medini P, Berardi N, Chierzi S, Fawcett JW, Maffei L. Reactivation of ocular dominance plasticity in the adult visual cortex with chondroitinase ABC. Science 2002; 298: 1248–51.

Pizzorusso T, Medini P, Landi S, Baldini S, Berardi N, Maffei L. Structural and functional recovery from early monocular deprivation in adult rats. Proc Natl Acad Sci USA 2006; 103: 8517–22.

Properzi F, Carulli D, Asher RA, Muir E, Camargo LM, van Kuppevelt TH, et al. Chondroitin 6-sulphate synthesis is up-regulated in injured CNS, induced by injury-related cytokines and enhanced in axon-growth inhibitory glia. Eur J Neurosci 2005; 21: 378–90.

Putignano E, Lonetti G, Cancedda L, Ratto G, Costa M, Maffei L, et al. Developmental downregulation of histone posttranslational modifications regulates visual cortical plasticity. Neuron 2007; 53: 747–59.

Reimers S, Hartlage-Rubsamen M, Bruckner G, Rossner S. Formation of perineuronal nets in organotypic mouse brain slice cultures is independent of neuronal glutamatergic activity. Eur J Neurosci 2007; 25: 2640–8.

Rhodes KE, Fawcett JW. Chondroitin sulphate proteoglycans: preventing plasticity or protecting the CNS? J Anat 2004; 204: 33–48.

Sale A, Maya Vetencourt JF, Medini P, Cenni MC, Baroncelli L, De PR, et al. Environmental enrichment in adulthood promotes amblyopia recovery through a reduction of intracortical inhibition. Nat Neurosci 2007; 10: 679–81.

Sato M, Stryker MP. Distinctive features of adult ocular dominance plasticity. J Neurosci 2008; 28: 10278–86.

Sawtell NB, Frenkel MY, Philpot BD, Nakazawa K, Tonegawa S, Bear MF. NMDA receptor-dependent ocular dominance plasticity in adult visual cortex. Neuron 2003; 38: 977–85.

Schweizer M, Streit WJ, Muller CM. Postnatal development and localization of an N-acetylgalactosamine containing glycoconjugate associated with nonpyramidal neurons in cat visual cortex. J Comp Neurol 1993; 329: 313–27.

Sengpiel F. The critical period. Curr Biol 2007; 17: R742–3.

Smith GB, Heynen AJ, Bear MF. Bidirectional synaptic mechanisms of ocular dominance plasticity in visual cortex. Philos Trans R Soc Lond B Biol Sci 2009; 364: 357–67.

Sugahara K, Mikami T, Uyama T, Mizuguchi S, Nomura K, Kitagawa H. Recent advances in the structural biology of chondroitin sulfate and dermatan sulfate. Curr Opin Struct Biol 2003; 13: 612–20.

Sugiyama S, Di Nardo AA, Aizawa S, Matsuo I, Volovitch M, Prochiantz A, et al. Experience-dependent transfer of Otx2 homeoprotein into the visual cortex activates postnatal plasticity. Cell 2008; 134: 508–20.

Tom VJ, Kadakia R, Santi L, Houle JD. Administration of chondroitinase ABC rostral or caudal to a spinal cord injury site promotes anatomical but not functional plasticity. J Neurotrauma 2009; 26: 2323–33.

Tropea D, Caleo M, Maffei L. Synergistic effects of brain-derived neurotrophic factor and chondroitinase ABC on retinal fiber sprouting after denervation of the superior colliculus in adult rats. J Neurosci 2003; 23: 7034–44.

Tropea D, Van WA, Sur M. Review. Molecular mechanisms of experience-dependent plasticity in visual cortex. Philos Trans R Soc Lond B Biol Sci 2009; 364: 341–55.

Vo T, Carulli D, Ehlert EME, Kwok JC, Asher RA, Fawcett JW, et al. The chemorepulsive axon guidance protein Semaphorin 3A is a constituent of perineuronal nets in the adult rodent brain. Soc Neurosci Abstr 2007; 585: 1.

Wang H, Katagiri Y, McCann TE, Unsworth E, Goldsmith P, Yu ZX, et al. Chondroitin-4-sulfation negatively regulates axonal guidance and growth. J Cell Sci 2008; 121: 3083–91.

Watanabe H, Yamada Y, Kimata K. Roles of aggrecan, a large chondroitin sulfate proteoglycan, in cartilage structure and function. J Biochem 1998; 124: 687–93.

Zimmermann DR, Dours-Zimmermann MT. Extracellular matrix of the central nervous system: from neglect to challenge. Histochem Cell Biol 2008; 130: 635–53.